Energy and angular distributions of backscattered electrons from the collision of 8-keV electrons with a thick tungsten target

R. K. Yadav and R. Shanker*
Atomic Physics Laboratory, Department of Physics, Banaras Hindu University, Varanasi 221 005, India
(Received 27 February 2004; published 3 November 2004)

The energy and angular distributions of backscattered electrons produced under impact of 8.0-keV electrons with a thick tungsten target are measured. The energy range of backscattered electrons is considered between 70 and 1700 eV. The angle of incidence α and the takeoff angle θ are chosen to have values $\alpha=0°$, 10°, and 20° and $\theta=110°$, 120°, and 130°, respectively. The energy distribution function exhibits two sharp peaks, which are found to appear at 216 and 548 eV. They are identified as Auger peaks of tungsten arising due to electron transitions 4*d*-6*s*6*p* and 4*s*-6*s*6*p*, respectively. The measured energy spectra are compared with two different theoretical models. The theoretical predictions are found to yield a good agreement with the experiment in the considered energy range of the backscattered electrons.

DOI: 10.1103/PhysRevA.70.052901 PACS number(s): 79.20.Fv, 79.90.+b, 79.20.Hx

I. INTRODUCTION

A number of experimental investigations have been reported in the literature for backscattering of electrons from solid targets with incident energies up to 5 keV [1–8]; the results of these works were found to show considerable inconsistencies among themselves. The theoretical treatment of this fundamental scattering process at low impact energies is complicated due to failure of the Born approximation and a lack of detailed knowledge of the atomic potentials. More exact experimental information about the macroscopic effect, especially the energy and the angular distributions of backscattered electrons, would be required to examine the validity of existing theories. It is therefore worthwhile to measure the backscattering coefficient and the energy distributions of electrons backscattered from a thick solid target at higher impact energies. The theoretical treatment of a backscattering process in that case may become straightforward (Archard [9], Everhart [10]) or may become extremely complex (Bishop [11], Brown *et al.* [12]). It is noted that the simple treatments give a good qualitative idea about the physical processes involved in the backscattering process but do not give an accurate quantitative description. The more complicated theories predict the backscattering coefficients "η" well but they are less accurate for the energy and the angular distributions spectra. They are, in addition, extremely laborious and must be evaluated numerically for each situation of interest. The experimental and the theoretical knowledge of the interaction between incident electrons of intermediate energies and complex atoms is still very limited in contrast to the situation where impact energies are very large or very small relative to the atomic binding energy of the target atom. Measurements of the energy and the angular distributions of electrons backscattered from solids at intermediate energies, such as those reported in this paper, are expected to give insight into the relative importance of backscattering and of elastic and inelastic processes. Aside from their practical interests, the data on backscattering process are also of value in improving and developing the theories on bremsstrahlung, cathodoluminescence, secondary emission, and on bombardment-induced conductivity, where information on the primary beam spreading and total energy loss in the material is required. At present, reliable data on the number of backscattered electrons exist only for a few elements for incident electrons having energies below 200 eV [13–16], between 200 and 2000 eV [17–20], and above 2000 eV [21–28]. The information on energy distribution of the backscattered electrons from solid targets is available only below 200 eV [29,30] and above 370 keV [31,32]. The investigation reported here was undertaken to see the effects of atomic binding energy on the scattering process. Measurements of the energy distribution of backscattered electrons from a thick tungsten target were carried out for electrons having a primary energy of 8000 eV. In these collisions, the energetic electrons are made to interact with a thick tungsten specimen at different incident angles α. Such interactions may induce ionization of inner atomic shells of the target atoms. Consequently, the highly excited atoms may relax either by an emission of a x-ray photon or by emission of an Auger electron.

In the past, the theoretical studies of energy distribution of backscattered electrons as a function of reduced energy $\varepsilon(=E/E_0)$ have been made for $\varepsilon=0-1$ by several workers [33–35]; at the same time the experimental investigations of this distribution have been also carried out by different workers [3,36–41]. Here, E and E_0 are the energies of backscattered and incident electrons, respectively. In the work reported here, the range of ε is limited between 0.009 and 0.213 due to the present experimental constraints. Hence the corresponding measured energy distribution of backscattered electrons lies in the energy range of 70–1700 eV. The two peaks appearing in the distribution are identified as Auger lines of tungsten whose intensities are studied as a function of the incidence and the takeoff angles (the takeoff angle is the angle between the direction of incident and that of ejected electrons). The present experiment is conducted with the advantage of a clean target, good vacuum, and a sensitive

*Corresponding author. Electronic address: rshanker@bhu.ac.in

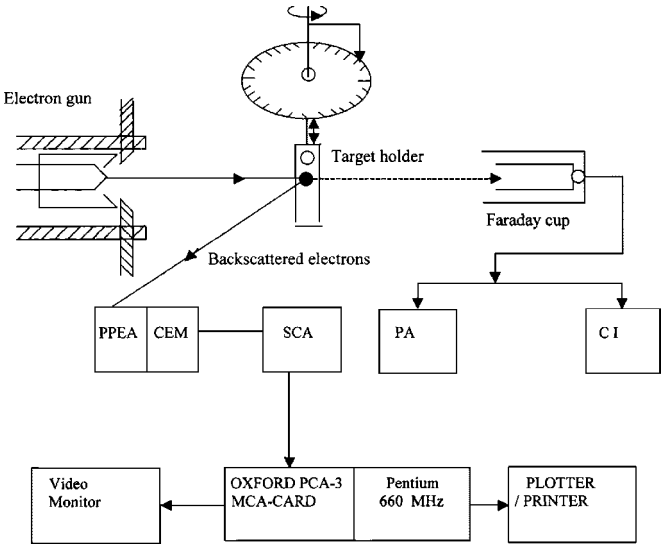

FIG. 1. Schematic diagram of the experimental setup: PPEA, parallel plate electrostatic analyzer; CEM, channel electron multiplier; SCA, single channel analyzer; PA, Pico ammeter; CI, current integrator.

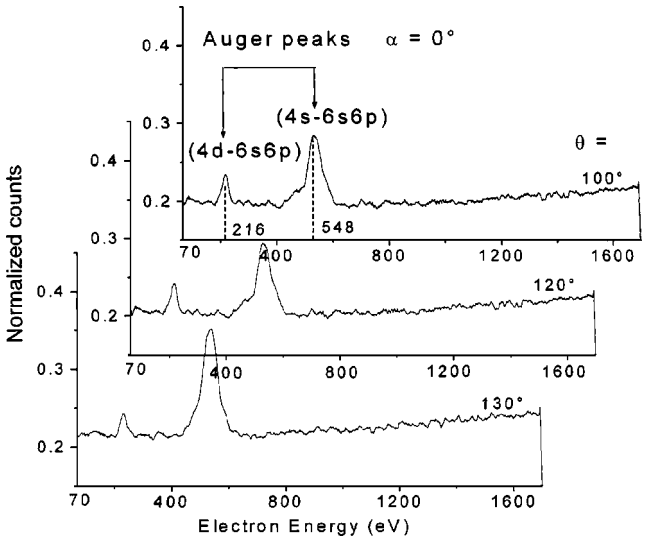

FIG. 2. Normalized counts as a function of the energy of backscattered electrons at 8-keV incidence energy, angle of incidence $\alpha=0°$ and takeoff angles $\theta=110°$, 120°, 130°.

and stable detection system that reveal a detectable fine structure in the energy spectra of backscattered electrons from the considered target.

II. EXPERIMENTAL METHOD

The measurements were carried out on a different experimental setup which is dedicated to the studies of electron-atom/molecule collision processes. Details of design and other aspects related to scattering chamber, detector, and electron source are discussed elsewhere [42]. The schematic diagram of the experimental set up is shown in Fig. 1. A monoenergetic beam of electrons was derived from a custom built electron gun (M/S P. Staib GmbH, Germany) which provided a focused beam of about 3 mm spot size at the target ($20\times14\times0.5$ mm) situated at about 500 mm away from the gun. The accuracy of positioning the beam spot on the target was estimated to be about ±1 mm. During measurements, the current of incident beam was kept at about 10 nA. The base pressure of the chamber was maintained at better than 1.6×10^{-6} Torr. The chamber is equipped with a movable target holder in the vertical plane at its center, which facilitates positioning the target in front of the beam. A high purity thick and polished tungsten target was mounted on the target holder. The backscattered electrons from the target were accepted with a narrow solid angle ($d\Omega=1.23$ sr) of a 45° parallel plate electrostatic analyzer (full width at half maximum=12%) equipped with a channel electron multiplier (CEM), which was operated in the pulse-counting mode. The energy spectra of backscattered electrons were measured as a function of the angle of incidence α and the takeoff angle θ. An elaborate description of signal processing, electronic circuit, data acquisition, and analysis, etc., has been given in Ref. [43]. The typical energy spectra of backscattered electrons from tungsten produced by collisions of 8-keV electrons are displayed in Figs. 2–4. The two well separated Auger peaks of tungsten arising due to the electron transitions $4d$-$6s6p$ and $4s$-$6s6p$ are clearly seen in the figures. The backscattering coefficient η is defined as a ratio of the current produced by the backscattered electrons on the plate (I_p) and the sum of the target current (I_t) and the plate current (I_p) that is, $\eta=I_p/(I_p+I_t)$. Uncertainty of measurements is believed to originate from two main sources; namely, fluctuations of the beam energy and integration of the beam current which are individually determined to be about ±1% and ±5%, respectively. Hence the total uncertainty of measurements for η is a little over ±5%. In all the above-mentioned experiments, the monitoring of the electron-beam current is accomplished by a Pico ammeter and the integration of electronic charges is done by a current

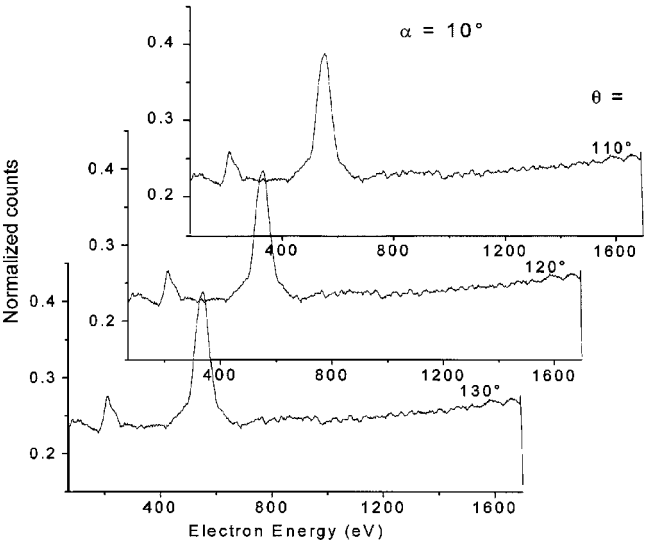

FIG. 3. Normalized counts as a function of the energy of backscattered electrons at 8-keV incidence energy, angle of incidence $\alpha=10°$ and takeoff angles $\theta=110°$, 120°, 130°.

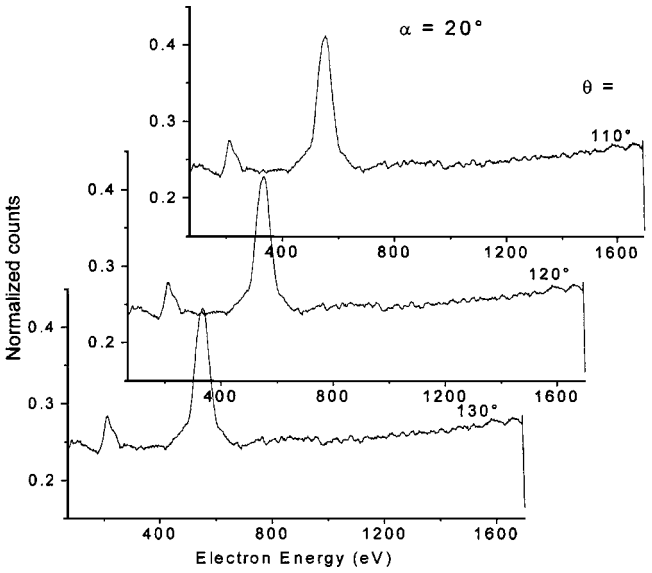

FIG. 4. Normalized counts as a function of the energy of backscattered electrons at 8-keV incidence energy, angle of incidence $\alpha=20°$ and takeoff angles $\theta=110°$, 120°, 130°.

integrator (EG&G, Ortec 439) for the normalization purposes.

III. THEORETICAL CONSIDERATION

The energy distribution of backscattered electrons from a pure and a mixed target has been studied theoretically using the Monte Carlo calculations by Matsukawa *et al.* [37]. Matsukawa *et al.* [38] have measured the energy spectra of backscattered electrons using a retarding potential technique for different elements ($Z=6$, 17, 29, 79) and for incidence energy of electrons of 20 keV. They have compared their experimental results with the Monte Carlo calculations for an angle of incidence $\alpha=0°$, and for fractions of energy ε for $\varepsilon=0-1$. They have shown that the theoretical calculations agree reasonably well with the experiment, although the theoretical curves overestimate the experimental data at higher values of ε, especially for heavy elements. Other experimental data at low impact energies are also available in the literature from several authors; for example, Sternglass [3], Kulenkampff and Spyra [4], Kanter [5], Kulenkampff and Ruttiger [6], Bishop [7], and Darlington [8]. It is, however, interesting to examine the energy distribution curves for backscattered electrons from thick targets of low and high Z elements obtained from those measurements which were carried out at high impact energies by other investigators. The only available data of this nature which lend themselves to a direct comparison are those of Brand [2] in the 16–32-keV energy region, and those of Bothe [44] at 370 and 680 keV; the earlier results of Wagner [45] are being more of a qualitative character. Brand's data were obtained for different directions of observation relative to the targets normal at impact energy of 16, 24, and 32 keV. Since the energy distributions vary with the takeoff angle θ, the comparison should be strictly made only for the same direction. Brand's corrected curves for incident energy of 32 keV indicate a surprising similarity to the data taken at much lower energies (0.5–2 keV) [3]. The change in shape of the distribution function with increasing atomic number Z is of the same character and areas under the curves of elements of the same or similar Z are shown to be approximately equal. The energy distribution curves at 370-keV energy given by Bothe show a much stronger change in the distribution with atomic number than the data available at lower energies. An examination of Bothe's plots reveals that for the heavy elements, for example, Pb ($Z=82$) and Sn ($Z=50$), there is a pronounced shift of the elastic peak towards the high-energy side.

In order to compare the present results with a theoretical prediction, particularly for a case of normal angle of incidence ($\alpha=0°$), we have considered, first, a theoretical model of McAfee [46] which is applicable for energy distribution of backscattered electrons only at $\alpha=0°$, is given as follows.

The backscattering coefficient η as a function of ε and Z is given as

$$\eta(\varepsilon,Z)=\frac{a-1-\varepsilon^2(a+1)+2\left[\frac{1}{2}(1+\varepsilon^2)\right]^{a+1}}{(1-\varepsilon^2)(a+1)}, \tag{1}$$

where $a=0.045Z$ (this is Everhart's adjusted value of a).

The energy spectra of the backscattered electrons can be calculated from Eq. (1) by computing $|d\eta(\varepsilon,Z)/d\varepsilon|$, which is obtained as

$$\frac{d\eta(\varepsilon,Z)}{d\varepsilon}=\frac{-4\varepsilon(a+1)+2\varepsilon(a+1)[2+a(1-\varepsilon^2)]\left[\frac{1}{2}(1+\varepsilon^2)\right]^a}{[(1-\varepsilon^2)(a+1)]^2}. \tag{2}$$

Since the data of the present measurements provide the double differential cross sections $[d^2\eta(\varepsilon,Z)/d\varepsilon d\Omega]$ of the backscattered electrons as a function of ε and $d\Omega$, we have to integrate these cross sections over the takeoff angles for obtaining the energy distribution function $[d\eta(\varepsilon,Z)/d\varepsilon]$, that is,

$$\int_{E=\pi/2}^{\pi}\frac{d^2\eta(\varepsilon,Z)}{d\varepsilon d\Omega}d\Omega;\ \phi=\pi-\theta;\ d\Omega=2\pi\sin\theta d\theta d\Phi$$

which yields the desired expression for energy distribution of backscattered electrons as

$$\frac{d\eta(\varepsilon,Z)}{d\varepsilon}=E_0\left[\frac{d\eta(\varepsilon,Z)}{dE}\right]. \tag{3}$$

Equation (3) represents the characteristics exhibited by Eq. (2).

Second, we have compared our data with the theoretical model of P-F Staub [39], which predicts the energy and the angular distributions of backscattered electrons. The energy spectra of backscattered electrons for an angle of incidence α in this model is given by

$$g(E/E_0) = -\frac{\partial \eta(E/E_0)}{\partial E}, \tag{4}$$

$$\eta(E/E_0) = S \exp\left[-\left(\frac{K}{1-\gamma(E/E_0)^{\delta}}\right)^{p}\right],$$

where S, K, p, γ, δ is a set of independent parameters

$$K = 70|\ln B|^4,$$

$$P = 0.27,$$

$\gamma = 1 - \exp(-6|\ln B|^{-3/2})$, $\delta = 2.0$. S is the normalization function,

$$S = B \exp[(K)^p],$$

where B is defined as $B_\alpha = B_0^{[1-k(1-\cos\alpha)]}$, where α is the angle of incidence and B_0 is the backscattering coefficient at normal incidence, which is defined in the energy interval $0.5 \leqslant E_0 \leqslant 30$ keV as

$$B_0 = \beta\{1 - \exp[(-6.6 \times 10^{-3})\beta^{-5/2}Z]\},$$

$\beta = 0.40 + 0.065 \ln E_0$, where E_0 is in keV,

$$k(E_0) = 1 - \exp(-1.83E_0^{1/4})$$

for $E_0 = 8$ keV, $k(E_0) = 0.95$.

The energy distributions of backscattered electrons are computed using Eqs. (2) and (4) which are shown in Fig. 6.

IV. RESULTS AND DISCUSSION

The energy spectra of backscattered electrons produced from collisions of 8-keV electrons with a thick tungsten target as a function of incidence angle $\alpha = 0°$, 10°, and 20° for different takeoff angles are shown in Figs. 2–4. These spectra were normalized with the total charge collected on the target during acquisition of the data for a given angle of incidence and takeoff angle. These spectra are found to show two distinct Auger peaks: the first one appearing at about 216 eV and the second at 548 eV, respectively. These peaks are attributed to Auger transitions: 4*d*-6*s*6*p* and 4*s*-6*s*6*p*, respectively. The theoretically calculated energies of these peaks are found to be, respectively, 207 and 552 eV [47]. The experimental and theoretical values of energy of these Auger peaks are thus seen to agree with each other within less than 5%. It is also noted that the full width at half maximum (FWHM) of each Auger peak is about 70 eV. However, the corresponding half intensity widths of the peaks determined from the present resolution of ESA are estimated to be 26 and 66 eV, respectively, which are less than the peak widths. This result indicates that the two peaks are originating from single Auger transitions as mentioned above. No shift is observed for the Auger peaks either with the angle of incidence or with the takeoff angle. The intensity of the peak is found to increase with the angle of incidence α at a fixed takeoff angle (see Figs. 2–4). This enhancement in intensity is due to the additional ionization of the inner shells of the target atoms by the backscattered electrons, which lose lesser energy in penetrating the target at larger incidence angles compared to that at a normal incidence ($\alpha = 0°$) by a factor of sec α [48]. The relative intensities of the peaks appearing, for example, for $\alpha = 0°$, 10°, and 20° at $\theta = 120°$ are in the ratio of 1.00:1.36:1.42. Further, it is also noted that for a fixed α and different takeoff angles, for example, $\theta = 110°$, 120°, and 130°, the relative intensity of the Auger peak increases with θ; this is because the backscattered electrons which suffer larger takeoff angles travel a smaller path in the target and lose lesser energy than those suffering smaller takeoff angles. For such a intensity distribution in the Auger peaks, attenuation of intensity may take place due to absorption of Auger electrons in the target materials. The loss of intensity due to this channel has not been taken into account in the present analysis. The backscattered electrons which are more energetic, are being capable of creating additional ionization events in the target atom. In the latter case, the relative intensities of the Auger peaks for $\alpha = 20°$ and at $\theta = 110°$, 120°, and 130° are in the ratio of 1.00:1.02:1.04 (see Fig. 4).

The production cross sections of backscattered electrons from a thick tungsten target by impact of 8.0-keV electrons were measured for $\alpha = 0°$, 110°, 120° and for $\theta = 110°$, 120°, 130° as a function of the energy of backscattered electrons. The results of these measurements are shown in Fig. 5. From this figure, it is seen that for a particular angle of incidence, the relative cross sections of backscattered electrons are found to increase slowly with the takeoff angle θ and with the energy of the backscattered electrons. The dashed lines in the figure represent the locations of the Auger peaks. The range of fraction of energy ($\varepsilon = E/E_0$) was considered from 0.009 to 0.213. It should be pointed out here that the range of variations of experimentally determined energy distribution curves or electron energy spectra in the published literature is surprisingly large and seems not to have been addressed fully down up to $\varepsilon = 0$. It is of passing interest (and is regarded as only coincidental) that the measured energy spectra obtained by Darlington and Cosslett [49] (their Fig. 10 and following) lies somewhat closer to the triangular shape obtained here than do others. However, in at least one figure their measured spectra for $E_0(d\eta/dE)$ appear to go to zero for a ε value somewhere between 0.25 and 0.50. One cannot be completely certain since these authors do not continue their curves down to lower values of ε. It would be very useful to have careful measurements of $\eta(\varepsilon, Z)$ for a given target and fixed E_0 with ε varying in small steps starting from zero up to the considered limit. Figure 6 shows the energy distributions $E_0(d\eta/dE)$ of backscattered electrons integrated over the takeoff angles θ as a function of ε. The cross sections of energy spectra of backscattered electrons for the large angle of incidence are seen to be relatively larger as compared for those at a low angle of incidence. The solid line and the dotted line curves shown in the figure represent the theoretical calculations using Eqs. (2) and (4), respectively. The filled circles are the present experimental data points. The comparison of the theoretical prediction with the experimental data is found to exhibit a satisfactory

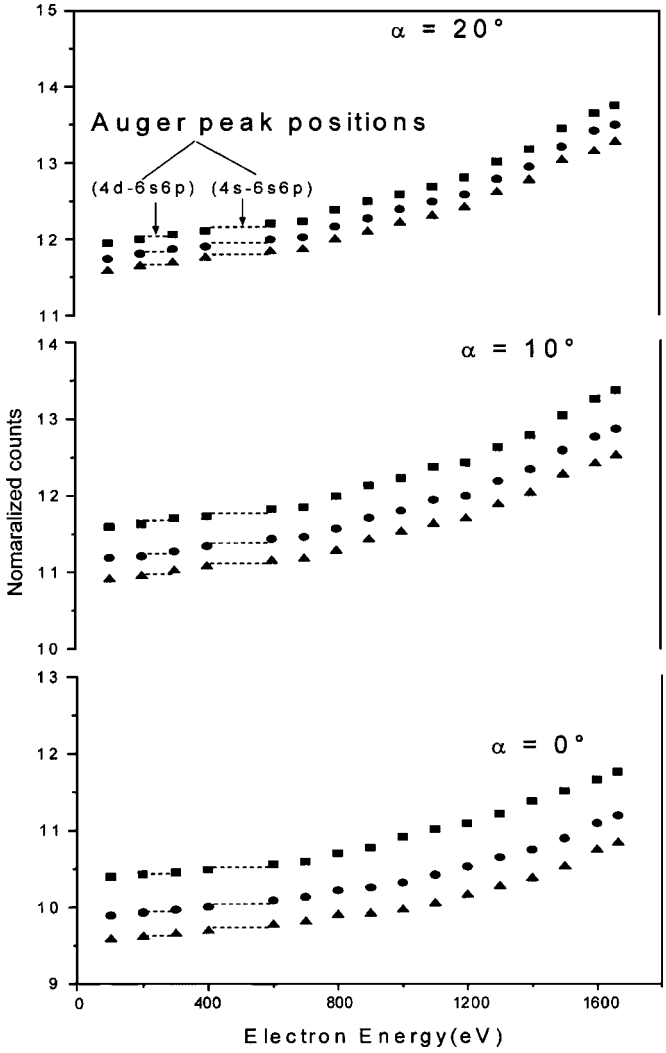

FIG. 5. Normalized counts as a function of the energy of backscattered electrons for $\alpha=0°$, 10°, 20°: (▲), $\theta=110°$: (●), $\theta=120°$: (■), $\theta=130°$.

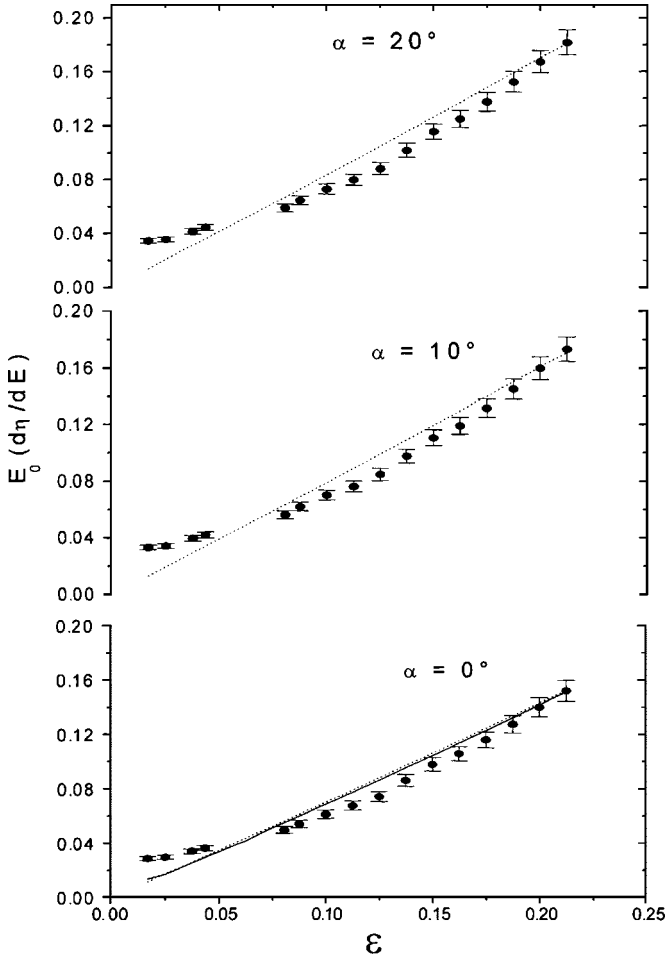

FIG. 6. Energy distributions of backscattered electrons from a thick tungsten target under impact of 8-keV electrons as a function of $\varepsilon=E/E_0$ and angle of incidence α for integrated takeoff angle θ. ●: present experiment, the solid and the dotted line curves are the theoretical results obtained using Eqs. (2) and (4), respectively.

agreement between them. In this comparison, the theory has been normalized to the experiment at $\varepsilon=0.213$. However, it is noted that both theories underestimate the data in the region corresponding to $\varepsilon\leqslant 0.05$. This may be explained due to the fact that in this region, most of the detected electrons are a mixture of true secondary ($E\leqslant 50$ eV), high-energy directly ejected (secondary) electrons in addition to the true backscattered electrons having energies $\leqslant 400$ eV. The secondary electrons are generally produced by primary as well as by backscattered electrons. However, the discriminated detection of genuine backscattered electrons is not possible in the present measurements. It is further seen that the value of $E_0(d\eta/dE)$ increases with the angle of incidence for a given value of ε. This occurs because the absorption of the backscattered electrons in the target at a low value of α is considerably larger than that at a larger α, as the path lengths traveled by these electrons in the target before reaching the surface are increased. Therefore the backscattered electrons measured at low α do not dominate the total backscattering cross sections despite their increased elastic scattering probability.

V. CONCLUSIONS

The present work deals with the measurements of energy and angular distributions of electrons backscattered from a thick tungsten target under impact of 8-keV electrons using a 45° parallel plate electrostatic analyzer. The energy spectra exhibit two distinct Auger peaks appearing at 216 and 548 eV. They are suggested to arise from electron transitions 4*d*-6*s*6*p* and 4*s*-6*s*6*p*, respectively. The variation of intensity of these peaks as a function of incidence and takeoff angles are studied. Further, the energy distribution of backscattered electrons as a function of ε is shown to increase with angle of incidence α for a given value of ε. Also, the cross sections of energy spectra for the large angle of incidence are found to be relatively larger than for those at low angle of incidence. The predictions of two theoretical models calculated using Eqs. (2) and (4) are found to be in a satisfactory agreement with our experiment, however, the theory is seen to underestimate the experiment for data corresponding to

$\varepsilon < 0.05$; this is explained due to the presence of secondary electrons in dominance over the backscattered electrons in this region. Nevertheless, overall agreement between experiment and theory suggests that in the considered range of ε, both theoretical models are found to predict a reasonable account of the energy distribution function.

ACKNOWLEDGMENTS

This work has been supported by the Department of Science and Technology (DST), New Delhi, under Research Project No. SP/S2/L-08/2001. The authors would like to thank S. Mondal and Argala Srivastava for their help in the experiments.

[1] H. E. Bishop, Br. J. Appl. Phys. **1**, 673 (1968).
[2] J. O. Brand, Ann. Phys. (Leipzig) **26**, 609 (1963).
[3] E. J. Sternglass, Phys. Rev. **95**, 345 (1954).
[4] H. Kulenkampff and Spyra, Z. Phys. **137**, 416 (1954).
[5] H. Kanter, Ann. Phys. (Leipzig) **20**, 144 (1957).
[6] H. Kulenkampff and K. Ruttiger, Z. Phys. **152**, 249 (1958).
[7] H. E. Bishop, Ph.D. thesis, University of Cambridge, 1966.
[8] E. H. Darlington, Ph.D. thesis, University of Cambridge, 1971.
[9] G. D. Archard, J. Appl. Phys. **32**, 1505 (1961).
[10] T. E. Everhart, J. Appl. Phys. **31**, 1483 (1960).
[11] H. E. Bishop, Br. J. Appl. Phys. **18**, 703 (1967).
[12] D. B. Brown, D. B. Wittry, and K. F. Kyser, J. Appl. Phys. **40**, 1627 (1969).
[13] H. Bruining, Physica (Amsterdam) **5**, 913 (1938).
[14] I. Gimpel and O. Richardson, Proc. R. Soc. London, Ser. A **182**, 17 (1943).
[15] O. Krenzien, Z. Phys. **126**, 365 (1949).
[16] H. P. Myers, Proc. R. Soc. London, Ser. A **215**, 329 (1952).
[17] C. M. Kwei, C. J. Hung, P. Su, and C. J. Tung, J. Phys. D **32**, 3122 (1999).
[18] A. Jablonski, Phys. Rev. B **43**, 7546 (1991).
[19] C. Robert, B. Gruzza, L. Bideux, and P. Bondot, Math. Comput. Simul. **47**, 419 (1998).
[20] B. Gruzza, C. Robert, B. Peuchot, and L. Bideux, Vacuum **50**, 237 (1998).
[21] P. Palluel, C. R. Hebd. Seances Acad. Sci. **224**, 1492 (1947).
[22] B. F. J. Schouland, Proc. R. Soc. London, Ser. A **104**, 235 (1923); **108**, 187 (1925).
[23] K. H. Stehberger, Ann. Phys. (Leipzig) **86**, 825 (1928).
[24] R. K. Singh and R. Shanker, J. Phys. D **31**, 2221 (1998).
[25] R. K. Yadav, Argala Srivastava, S. Mondal, and R. Shanker, J. Phys. D **36**, 2538 (2003).
[26] A. M. D. Assad and M. M. ElGomati, Scanning Microsc. **12**, 185 (1998).
[27] M. Dapor, Phys. Rev. B **46**, 618 (1992).
[28] J. W. Martin, J. Yuan, S. A. Hoedl, B. W. Filippone, D. Fong, T. M. Ito, E. Lin, B. Tipton, and A. R. Young, Phys. Rev. C **68**, 055503 (2003).
[29] H. W. Farnsworth, Phys. Rev. **31**, 405 (1928).
[30] E. Rudberg, Phys. Rev. **50**, 138 (1936).
[31] W. Bothe, Z. Naturforsch. B **40**, 542 (1949).
[32] J. O. Brand, Ann. Phys. (Leipzig) **26**, 609 (1936).
[33] M. Andrae, K. Rohrbacher, P. Klein, and J. Wernisch, Scanning **18**, 401 (1996).
[34] B. Gruzza, C. Robert, L. Bideux, B. Peuchot, and A. Jablonski, J. Surf. Anal. **5**, 90 (1999).
[35] Z. J. Ding, Int. J. Mod. Phys. B **16**, 4405 (2002).
[36] E. H. Darlington, J. Phys. D **8**, 85 (1975).
[37] T. Matsukawa, K. Murata, and R. Schimizu, Phys. Status Solidi B **55**, 371 (1973).
[38] T. Matsukawa, R. Shimizu, and H. Hashimoto, J. Phys. D **7**, 95 (1974).
[39] P-F. Staub, J. Phys. D **27**, 1533 (1994).
[40] P. Gerard, J. L. Balladore, J. P. Martinez, and A. Ouabbou, Scanning **17**, 377 (1995).
[41] D. Berger and H. Niedrig, Scanning **24**, 70 (2002).
[42] R. K. Singh, R. K. Mohanta, R. Hippler, and R. Shanker, Pramana, J. Phys. **58**, 499 (2002).
[43] R. K. Singh, R. Hippler, and R. Shanker, J. Phys. B **35**, 3243 (2002).
[44] W. Bothe, Z. Naturforsch. B **49**, 542 (1949).
[45] P. B. Wagner, Phys. Rev. **35**, 98 (1930).
[46] W. S. McAfee, J. Appl. Phys. **47**, 1179 (1976).
[47] G. A. Harrower, Phys. Rev. **102**, 340 (1956).
[48] T. E. Gallon, J. Phys. D **5**, 823 (1972).
[49] E. H. Darlington and V. E. Cosslett, J. Phys. D **5**, 1969 (1972).